Journal of the European Ceramic Society 36 (2016) 3185–3191

Contents lists available at www.sciencedirect.com

Journal of the European Ceramic Society

journal homepage: www.elsevier.com/locate/jeurceramsoc

Tensile strength distribution of all-oxide ceramic matrix mini-composites with porous alumina matrix phase

Henning Richter*, Piet W.M. Peters

Institute of Materials Research, German Aerospace Center (DLR), Linder Hoehe, 51147 Köln, Germany

ARTICLE INFO

Article history:
Received 21 March 2016
Received in revised form 3 May 2016
Accepted 6 May 2016
Available online 17 May 2016

Keywords:
Ceramic-matrix composites (CMCs)
Mechanical testing
Tensile strength
Statistical properties
Microstructure

ABSTRACT

The mechanical behaviour of all-oxide ceramic matrix mini-composites with porous alumina matrix phase was investigated by performing uniaxial tensile tests on specimens with different gauge lengths. The specimens were fabricated from Nextel™ 610 fibres by slurry infiltration and subsequent sintering at 1300 °C for 1 h.

The stress–strain curves of the tested mini-composites revealed that the porous alumina matrix phase accumulates damage with increasing tensile load, but continues to contribute to the mini-composites' tensile stiffness until ultimate failure occurs. A dependence of the tested mini-composites' axial tensile strength on gauge length was not observed. The mean stress in the fibres at mini-composite failure was found to decrease with increasing matrix volume fraction, indicating that the cause of ultimate failure of the mini-composites can be attributed to the propagation of matrix cracks.

1. Introduction

Owing to their fracture toughness, heat and oxidation resistance, as well as low specific weight, all-oxide ceramic matrix composites (CMCs), which typically consist of alumina or aluminosilicate fibre bundles embedded in a porous, alumina- or aluminosilicate-based matrix, are promising materials for high-temperature applications under oxidizing conditions. The non-linear structural behaviour exhibited by all-oxide CMC components with multi-directional fibre orientation under fibre-nonparallel mechanical loading results from the interplay of damage and failure processes acting at several material length scales. The CMC components' overall performance is strongly influenced by the mechanical properties of the unidirectional fibre bundles, which constitute the smallest repetitive mechanical entity discernible in all-oxide CMCs [1,2].

Generally, the mechanical behaviour of the fibre bundles in all-oxide CMCs differs fundamentally from that found in conventional, polymer-based unidirectional composites. In the latter, the ductile matrix phase exhibits high strain-to-failure but low strength. The embedded fibres primarily stiffen and reinforce the polymer matrix. The axial tensile strength of the fibre bundles depends on the statistical strength properties of the fibres, the shear properties of the matrix phase and the fibre-matrix bond strength [3–7]. The damage process under tensile loading is characterized by matrix yielding, successive fibre rupture and load transfer between fractured and intact fibre segments [6,8].

In all-oxide CMCs, however, the brittle porous matrix phase generally has low strain-to-failure and comparatively low strength [9,10]. The embedded fibres primarily toughen the porous matrix phase [11,12]. The axial tensile strength of the fibre bundles in a ceramic matrix is commonly reported to be influenced by fibre strength statistics [13–16] and fibre-matrix debonding resistance [1,2,17–20].

While a multitude of micromechanical models describing the damage and failure behaviour of CMCs have been described in literature [21–32], published experimental data on the strength properties of unidirectional ceramic fibre bundles embedded in a brittle ceramic matrix, so-called ceramic matrix mini-composites, is scarce [28,33–35], especially for all-oxide ceramic matrix mini-composites [36].

This paper aims at contributing to the experimental background by reporting on the results of uniaxial tensile tests on all-oxide ceramic matrix mini-composites consisting of Nextel™ 610 alumina fibres [37] embedded in an alumina matrix phase with more than 30 vol% matrix porosity. A total of 90 mini-composites with three different gauge lengths were tested to investigate whether the mini-composites' axial tensile strength exhibits a dependence on gauge length. The obtained strength data and the stress–strain curves of the tested mini-composites were analysed to evaluate the mini-composites' damage and failure behaviour.

* Corresponding author.
E-mail address: henning.richter@dlr.de (H. Richter).

http://dx.doi.org/10.1016/j.jeurceramsoc.2016.05.012
0955-2219/

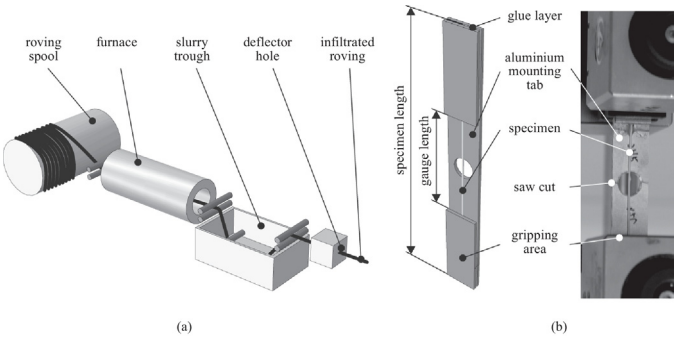

Fig. 1. Schematic processing route of unidirectional all-oxide ceramic matrix mini-composites (a), mounting tab geometry used for mechanical testing (b).

2. Experimental

2.1. Specimen preparation

The investigated ceramic matrix mini-composites were manufactured using a Nextel™ 610 fibre roving with a linear mass density of 3000 den, which corresponds to a nominal filament count of 750 [37], and an aqueous ceramic slurry of α-Al_2O_3 particles with an average particle size of approximately 200 nm prepared from PURAL® boehmite powder [38,39]. During manufacturing of the mini-composites, the as-received fibre roving was passed through a furnace to remove the organic sizing, infiltrated with the ceramic slurry and fed through a deflector with an opening of 1 mm in diameter to remove excess slurry. This manufacturing procedure, which is schematically shown in Fig. 1(a), is similar to the standard processing route of WHIPOX® components [40]. The infiltrated roving was manually cut into 18 bundle sections with lengths varying from approximately 800 mm to 1400 mm, which were then air dried for several hours. From each of the six shortest bundle sections, one set, and from each of the remaining 12 bundle sections, two sets of three tensile test specimens with nominal gauge lengths l_g = 50 mm, 125 mm and 250 mm were cut, yielding a total of n = 30 specimens per gauge length. All specimens were sintered for 1 h at a temperature of 1300 °C in air. The resulting matrix phase exhibits high porosity and more than 99.8 wt% alumina content.

After sintering, the mass and overall length of each specimen were recorded. Using Archimedes' principle, the density of one specimen from each of the 18 bundle sections was determined. This density was assumed to be representative for all specimens cut from the respective bundle section. With the known mass, density and overall length, the volume V and the average cross-sectional area A_c of each mini-composite specimen were computed.

The specimens were glued on 2 mm thick aluminium mounting tabs using a two-part epoxy adhesive, cf. Fig. 1(b), in order to facilitate handling and clamping, as well as to achieve, during mechanical testing, a gradual transfer of load from the clamped mounting tab to the specimen through shearing of the glue layer. The length of each gripping area was 40 mm.

2.2. Mechanical testing

Uniaxial tensile tests were carried out according to ASTM standards C1275-10 and C1557-03 [41,42] on a dual-column Instron 5566A testing machine equipped with a 500N load cell in a controlled environment at a temperature between 21 °C and 22 °C, a relative humidity between 50% and 60% and 984 hPa to 997 hPa ambient pressure.

During each test cycle, the mounted test specimen was positioned between the serrated grip faces and carefully aligned with marks on the grips in order to prevent spurious bending or torsion of the specimen. After clamping, the mounting tab was cut at the central drill-hole, cf. Fig. 1(b). Although care was taken to avoid damaging the fibre bundle surface, three specimens were destroyed during this process. Each tensile test was conducted at a constant nominal strain rate of approximately 10^{-4} s^{-1} to achieve fracture of the specimen within 20 s [42]. In the course of each test, the force F and the cross-head displacement u were recorded.

The cross-head displacement was used to estimate the specimens' tensile strain ε: to compensate for the compliance of the grips and other components in the load train, an effective gauge length l_e was determined from an additional tensile test on an as-received fibre roving embedded in epoxy resin, with a nominal gauge length of 50 mm. Neglecting the comparatively low Young's modulus of the epoxy matrix, the gauge length of the specimen was adjusted during analysis of the test result until the slope of the linear region of the stress–strain curve matched the known Young's modulus of the fibres [37], yielding an effective gauge length of l_e = 59.18 mm. Assuming the added compensation of 9.18 mm to be independent of the specimens' nominal gauge length, the effective gauge lengths l_e of the longer specimens were determined to be 134.18 mm and 259.18 mm, respectively.

2.3. Microscopy

After mechanical testing, a polished cross-section was prepared from each of the 18 bundle sections at a random location in order to determine the actual number n_f of fibres in the tested specimens. The individual fibres were counted on digital images obtained by scanning electron microscopy. Assuming the number of fibres to remain constant along the length of a bundle section, the fibre volume fraction φ and the matrix porosity ϕ_m of each specimen were computed from the number of fibres and the specimen length and volume for an average fibre diameter of 11.8 μm [43]. The digital images of polished cross-sections were further submitted to area measurements, using the ImageJ image analysis toolbox [44].

3. Results and discussion

3.1. Specimen microstructure

Actual fibre counts n_f of the 18 bundle sections ranged from 633 to 748. The fluctuation in fibre count is attributed to the rupture of individual filaments during manufacturing. The resulting fibre volume fraction φ of the mini-composites was found to vary from 12.8 vol% to 44.1 vol%, and matrix porosity ϕ_m was found to be in the range of 33.1 vol% to 43.1 vol%.

The digital area measurements confirmed the results derived from Archimedes density measurements, indicating that the variation in average cross-sectional area A_c along the length of the individual bundle sections is minimized by using the deflector to remove excess matrix slurry. However, a variation in diameter among different bundle sections occurred despite using the deflector, and some bundle sections exhibit a diameter that is notably smaller than the deflector opening.

3.2. Screening for outlying data

Due to the pronounced scatter in measured load at failure data, prior to further analyses, the test results for each nominal gauge length were separately scanned for erroneous, outlying data using the maximum normed residual criterion [45–47]. For each set of load at failure data F_{b_i}, $i = 1, 2, \ldots, n$, where the sample size n indicates the number of successfully tested specimens, cf. Section 2.2,